International Journal of Material Forming (2024) 17:28
https://doi.org/10.1007/s12289-024-01827-x

ORIGINAL RESEARCH

Rotary compression test for determination of critical value of hybrid damage criterion for railway steel EA1T

Łukasz Wójcik[1] · Tomasz Bulzak[1] · Konrad Lis[1] · Grzegorz Winiarski[1] · Tomasz Kusiak[1]

Received: 12 October 2023 / Accepted: 28 March 2024 / Published online: 17 April 2024

Abstract

The article presents and discusses the problem of determining and characterizing the cracking limits of cross-rolled specimens. The limit values were determined in accordance with the hybrid Pater criterion. For the study, the author's test method was used, which allows the determination of the cracking moment, formed as a result of the Mannesmann effect during the compression of specimens in the channel. In order to determine the values needed to describe the cracking criterion, it was necessary to perform laboratory tests and numerical simulations of the process of compression in the channel of discs made of EA1T steel under hot forming conditions. Experimental tests were carried out for forming processes at 950 °C, 1050 °C and 1150 °C. The tested material had a disc shape with a diameter of 40 mm and a length of 20 mm, during the pressing process the diameter of the disc was reduced to a diameter of 38 mm. The increase in forming temperature caused a significant increase in the forming path until cracking occurred. Numerical tests were carried out in the finite element calculation environment Simufact.Forming 2021. The stress and strain distributions in the specimen axis were analysed during the tests, which were then used to calculate the hybrid cracking criterion limit according to Pater. After calculations according to the Pater criterion and after statistical analysis, the cracking criterion limits were obtained.

Keywords Ball stud · Ball pin · Cross wedge rolling · Railway steel · Damage criterion

Introduction

In the world, one of the largest land transport branches is rail transport, in which three sub-sectors are classified. The first subsector is passenger rail travel, the second is freight rail transport, while the last subsector includes rail transport infrastructure. The development of railroads is increasing the demand for the manufacture of components and parts needed for railroad bogies. Railroad bogies (bogies) are the basic assembly of the bogie chassis of a rail vehicle. Its design allows the vehicle to move in accordance with the course of the tracks [1–3].Railroad bogies are built from a number of components, which include assemblies of elements, i.e. wagon axles, frame, suspension. Wagon axles are the main sub-assembly of a railroad bogie, they are large-scale products manufactured in large series [4, 5]. Axles used in railroads are made as a solid monolithic component or as a hollow component [4, 6]. Hollow axles are used to reduce the weight of a vehicle, but due to the complicated manufacturing process (design and production) they are mainly used in high-speed rail vehicles [7–9].

Monolithic axes are most often produced by the open die forging method [1, 7], in which steel ingots of EA1T grade steel are used as ingots. The ingots obtained by the continuous casting method are subjected to a forging process to give a rough shape to the axle, which is then subjected to machining after cooling and appropriate heat treatment to obtain the target shape of the finished product. The forging process of railroad axles, has the advantage of stability in the production of axles, the microstructure

✉ Łukasz Wójcik
l.wojcik@pollub.pl

Tomasz Bulzak
t.bulzak@pollub.pl

Konrad Lis
k.lis@pollub.pl

Grzegorz Winiarski
g.winiarski@pollub.pl

Tomasz Kusiak
t.kusiak@pollub.pl

[1] Mechanical Department of Metal Forming, Lublin University of Technology, Nadbystrzycka 38D, Lublin 20-618, Poland

is well ground, but such a manufacturing process also has some disadvantages, i.e. a large amount of technological surplus (waste of material) and low production efficiency [10–13].

In recent years, research has been carried out on the shaping of solid and hollow railroad axles by cross-wedge rolling and computer numerical control (CNC) skew rolling methods [8].

Cross-wedge rolling is one of the new methods for manufacturing weighted axles. Cross-wedge rolling, compared with free forging processes, is characterized by lower consumption of materials and energy required for axle production [5, 14]. On the other hand, the main disadvantage of cross-wedge rolling processes for wagon axles is the overall size of machines and tools in the case of roller tools as well as flat tools [15].

Numerically controlled skew rolling technology is the latest development in the forming of wagon axles. Computer support of oblique rolling processes in is one of the most favourable methods of forming, as it allows to increase productivity relative to cross-wedge rolling and forging [16].

During the forming of wagon axles by rolling methods (cross-wedge rolling, CNC skew rolling), one of the constraints that affects the safety of axle operation is the formation of micro-cracks and cracking along the axis of the rolled component. Such defects subjected to loads during operation can cause damage [17–20]. . Therefore, the analysis of the pattern of crack formation and the evaluation of the estimation of the probability of cracking during rolling is crucial to the safety of rolling stock.

The models used to predict cracking in the case of plastically formed material are developed on the basis of various cracking criteria [15]. The fundamental aim of the criteria is to predict the location of cracking occurrence and to determine the critical failure value cracking criteria are such as:: Freu-denthal, Cockroft - Latham, Oh, Brozzo et al., Ayada, Oyane, Zhan et al., Rice&Tracey, Argon et al. [21–25].

In contrast, several methods are used in the numerical modelling by finite element method (FEM) of cross-wedge rolling [26–28]. By correctly predicting the cracking of the forming material, cracking can be eliminated at an early stage in the design of the cross-wedge rolling process. The first criterion used because the study of the CWR was presented by Zhou's research team [29] presented a criterion according to which cracking of the forming material in the cross-wedge rolling process will occur if its value is greater than or equal to the limit value. The article [30] presents an FEM computation based on Zhou's study, where the author found that the criterion presented by Zhou shows the highest values in the initial phase of the test, but at this point no cracking is initiated, while when cracking occurs the value of this criterion is the lowest. The criterion is represented by a mathematical formula:

$$f = A\tau_{max} + B\sigma_1 \tag{1}$$

where:

f failure criterion value

τ_{Max} maximum shear stress

σ_1 maximum principal stress

A, B material constants

In a subsequent paper [31], Zhou proposed a new updated version of the criterion that can be used for highly ductile materials. The new criterion is an energy criterion that takes into account the accumulation of plastic deformation just before cracking of the forming material is initiated.

A literature review concluded that the first Zhou criterion is only applicable to materials with low ductility, while the second criterion does not allow the determination of the material constant C which limits the application of the criterion to the prediction of cracking in the CWR process.,

A third criterion for determining when cracking occurs during the rolling process is the hybrid criterion according to Pater [16]. The hybrid fracture criterion according to Pater was established on the basis of two criteria: the ductile fracture criterion and the maximum shear stress criterion. Pater adopted as the ductile cracking criterion the most commonly used criterion, the normalised Cockroft-Latham criterion, and referred to pure plastic shear stress using the Huber-Mises hypothesis. The hybrid cracking criterion according to Pater is described by Eq. (2).

$$f_{PATER} = \int_0^{\varepsilon} \left[(1-\Phi)\frac{\sqrt{3}}{2}\frac{\sigma_1-\sigma_3}{\sigma_z} + \Phi\frac{\sigma_1}{\sigma_z} \right] d\varepsilon \quad \begin{Bmatrix} \Phi = 0 \text{ dla } \eta \le 0, \\ \Phi = 3\eta \text{ dla } 0 < \eta \le 0{,}333, \\ \Phi = 1 \text{ dla } \eta > 0{,}333. \end{Bmatrix} \tag{2}$$

where

σ_1 maximum principal stress

σ_3 minimum principal stress

σ_z effective stress

ε effective strain

Φ coefficient describing the fraction of ductile fracture in the damage function

The aim of the developed study is to examine the EA1T material used in the manufacture of wagon axles in terms of predicting unwanted cracking inside the wagon axle forgings using the hybrid Pater criterion. The Pater criterion was used because of its good applicability to cross-wedge rolling processes.

Materials and methods

This paper presents the results of a cracking criterion study according to the hybrid Pater criterion hypothesis of EA1T steel. The analysed EA1T steel is an unalloyed quality steel, which is the most commonly used for the production of wagon axles. EA1T steel is characterized by high strength, high wear resistance and fatigue resistance. EA1T can withstand high loads, speeds and temperatures. To achieve the right properties, EA1T steel undergoes a special heat treatment process including quenching and tempering. The heat treatment process can improve microstructure, hardness and mechanical properties. Table 1 shows the chemical composition of EA1T steel.

In calculating the values needed to describe the cracking criterion according to Pater's hybrid cracking criterion, it was necessary to carry out laboratory tests and numerical simulations of the process of rotary compression of a disc-shaped specimen in a channel. The discs were made of EA1T steel under hot forming conditions.

The laboratory test method used is to determine the moment of cracking, which is caused by the Mannesmann effect during the forming process in the channel. In the adopted test method, the charge is a steel disc with a diameter of 40 mm and a height of 20 mm heated to temperatures of 950 °C, 1050 °C and 1150 °C in an electric chamber furnace. The heated charge is placed in a channel of width b at a distance S from the end of the lower tool. Then the upper tool, performing a linear motion at a constant speed v along the lower tool, is forming a disc with an initial diameter of D = 40 mm to a final diameter of 2 h = 38 mm, the lower tool remains stationary. The use of the channel causes its side walls to prevent axial expansion of the material, as a result of which the disc is subjected to varying compressive-tensile stresses, promoting the formation of axial cracking inside the formed disc. The principle of operation of the rotary compression method used in the channel is shown in Fig. 1.

To carry out laboratory tests of rotary compression in the channel, a laboratory cross-wedge rolling mill with tools in the form of a flat cross-wedge plate is shown in Fig. 2a. The rolling mill used is characterized by the fact that only the upper tool performs uniform motion at a constant speed of 300 mm/s, while the lower tool remains stationary. The tools used have the following dimensions: width 310 mm and length 1000 mm. Studies of rotary compression of a rotary disc in a channel were carried out using flat tools with a channel along the plate, the tools are shown in Fig. 2b.

Experimental studies of rotary compression in the channel of a disc of EA1T steel were carried out in a way to determine the exact path along which cracking of the specimen will occur. In the first stage, experiments were performed with a large step of the path S with the aim of roughly determining the path leading to cracking. Then, in terms of the path along which cracking occurred, the number of samples was concentrated so as to determine the moment just before cracking occurred. Once this moment

Table 1 Chemical composition of EA1T steel

Element	Share %
C	0,32–0,39
Cr	≤0,40
Cr + Mo + Ni	≤0,63
Mn	0,5 – 0,8
Mo	≤0,1
Ni	≤0,4
P	≤0,045
S	≤0,045
Si	≤0,4

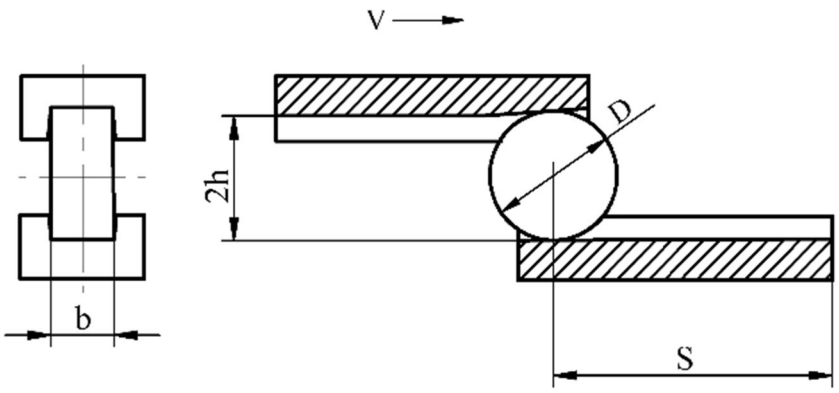

Fig. 1 Scheme of the working principle of the rotary compression method in the canal

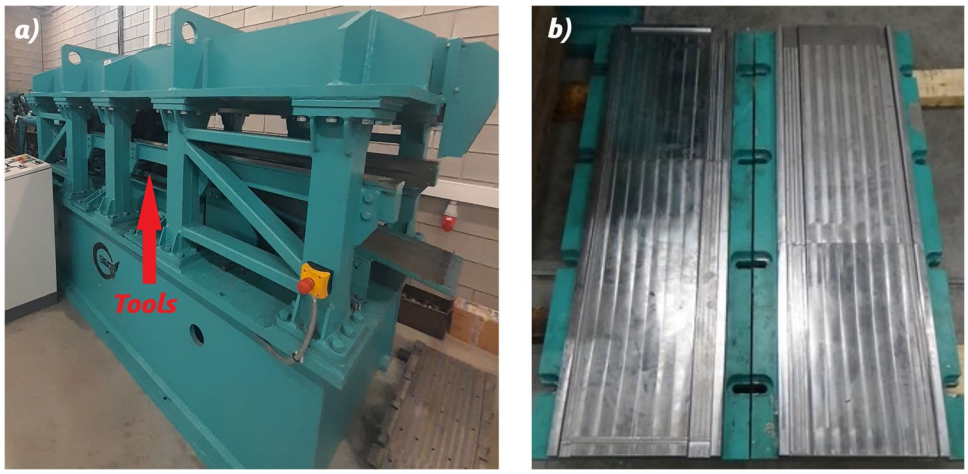

Fig. 2 Test stand: **a** laboratory cross and wedge rolling mill, **b** tools used for tests

was determined, two more tests (3 in total) were performed to verify the correct determination of the critical path value. If no cracking occurred after performing three rolling tests, the S-road was considered the value wanted.

After laboratory testing, numerical simulations were performed in SIMUFACT.FORMING 2021 software. To perform FEM simulation, it was necessary to model the channel tools and the disc charge.

For the FEM simulation, a top tool and a bottom tool were designed with a channel 20 mm wide and 1000 mm long and a side wall angle of 5°. Figure 3 shows a view of the tools and the batch in the start position and end position of the FEM simulation. The top tool is red, the bottom tool is blue, and the workpiece is pink.

Results

After conducting laboratory tests and then numerical tests of the rotary compression process in the channel of a disc made of EA1T steel, an analysis of the obtained results was carried out.

Laboratory tests were conducted under hot forming conditions. Rotary compression of discs was carried out at 950 °C, 1050 °C and 1150 °C. During the laboratory tests, the progression of the change in the shape of the specimen and the temperature during the rotary compression process was recorded. Figures 4, 5 and 6 show the progression of shape change of the rolled discs.

Based on the results of laboratory tests of rotary compression of specimens in the channel, the limits of the forming path and the corresponding number of specimen rotations were determined. For specimens made of EA1T steel (Fig. 7) forming at 950 °C, cracking inside the specimen was obtained after a distance of 170 mm. In the case of forming at 1050 °C, cracking occurred after a path of 200 mm, while for 1150 °C the limiting value of the forming path was 500 mm.

Experimentally determining the limit value of the path S after which cracking occurs inside the specimen, allowed us to determine the limit value of specimen rotation until cracking occurs. The limiting value of rotation was determined based on Eq. (3). Meanwhile, the results of the calculations are shown in Table 2 and Fig. 8.

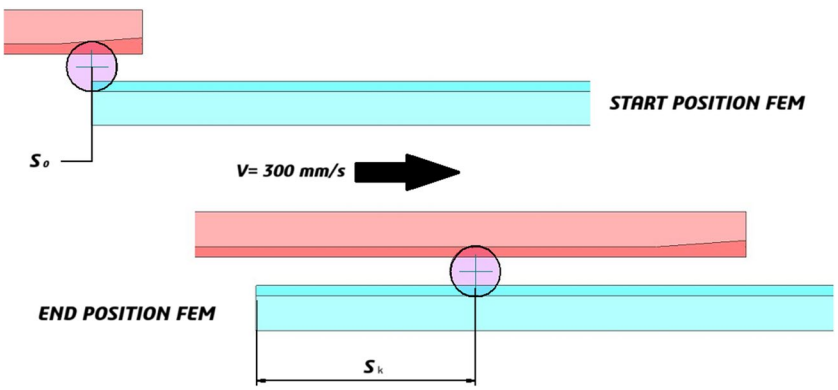

Fig. 3 Tool and workpiece models in the start and end positions of the FEM simulation

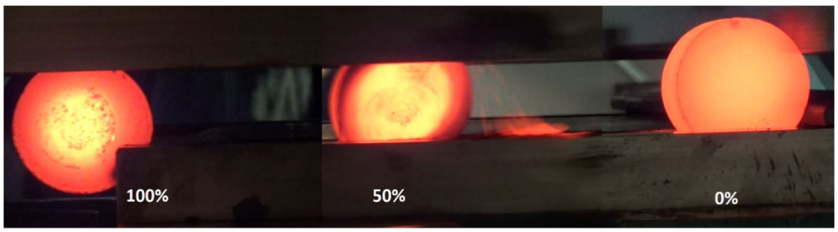

Fig. 4 Progression of the shape of a specimen forming at 950 °C

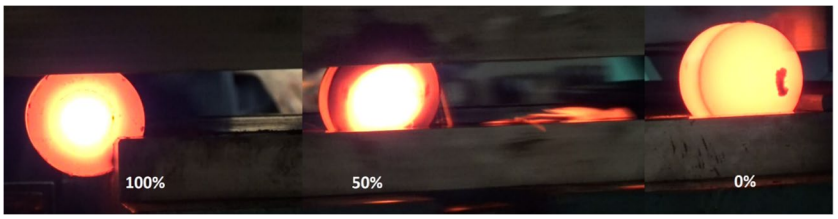

Fig. 5 Progression of the shape of a specimen forming at 1050 °C

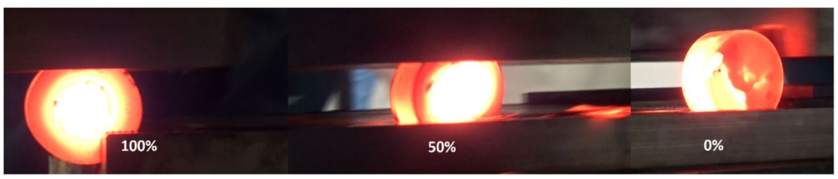

Fig. 6 Progression of the shape of a specimen forming at 1150 °C

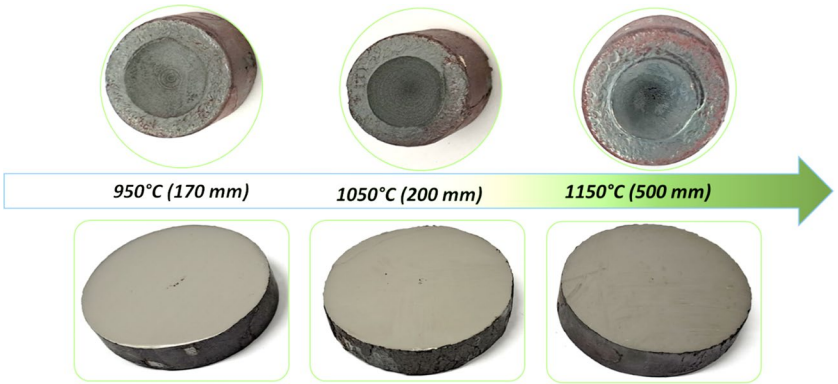

Fig. 7 View of samples after laboratory testing

Table 2 Limit number of specimen rotations leading to material cracking

Temperature	950 °C	1050 °C	1150 °C
Limit number of rotations	1.35	1.59	3.98

$$n = \frac{S}{\pi D_0} \tag{3}$$

where

S limiting distance [mm]

D_0 initial diameter of the forming specimen [mm]

During the forming of the specimens, the distribution of temperature values of the rotary compression specimens in the channel was analysed. Figure 9 shows maps of temperature distributions obtained from measurements with a FLIR thermal imaging camera, which in the next step were used to compare the results with computer simulation.

Based on the laboratory results obtained, numerical FEM simulations were carried out using Simufact.Forming 2021 software. Numerical tests were carried out for forming the disc to a path with a limit value for each temperature, accordingly. The material model used for the tests was assumed from the material library implemented by the manufacturer in the calculation software.

The workpiece was modelled as a disc with the same dimensions as the sample used for laboratory testing. A

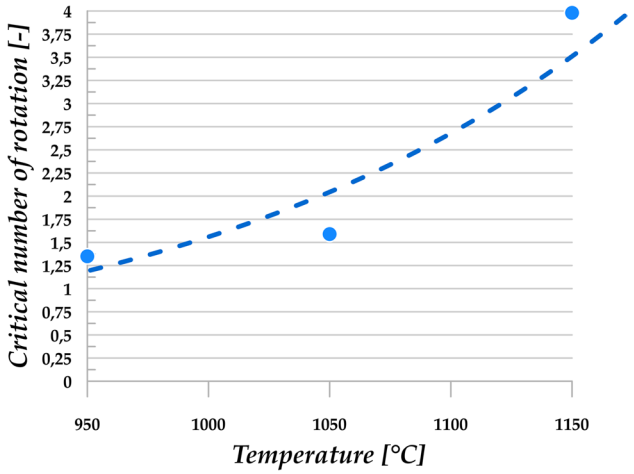

Fig. 8 Graph of the change in the limit number of turns for EA1T steel

hexagonal FEM mesh constructed of 13,382 elements of 1.25 mm in size was superimposed on the charge model. Figure 10 shows the FEM mesh used for the calculations.

Next, 21 points (measuring sensors) were placed on the batch model in the axis of rotation at a distance of 2 mm, as shown in Fig. 11.

The measurement points used aim to check the values of the various parameters tested needed to determine the value of the cracking criterion according to Pater's hybrid hypothesis.

To correctly carry out the computer simulation, boundary conditions corresponding to the laboratory tests carried out were used. The speed of the upper tool was assumed to be 300 mm/s, while the speed of the lower tool was set at 0 mm/s due to the design of the laboratory rolling mill. The friction factor between the forming material and the steel tools was assumed m = 0.99, while the tool temperature was assumed 20 °C. the temperature of the test specimens was assumed 950 °C, 1050 °C, 1150 °C with an applied heat transfer coefficient of 2000 W/(m^{2}K).

The numerical analysis made it possible to determine maps of the distributions of σ_1, σ_3, σ_z, ε and the triaxial stress state. Shape progression obtained by numerical analysis is presented, too (Fig. 12). Qualitatively comparing the shape of the specimen obtained in laboratory tests and the shape of the specimen obtained by the numerical testing process, a very high degree of similarity was determined.

On the basis of the numerical tests carried out, the temperature distributions (Fig. 13) were determined during the forming process on the surface and inside the sample. After mapping the temperature distributions, it was observed that on the surface of the sample forming at 950 °C, the maximum temperature obtained in both cases oscillated at around 825 °C, the maximum temperature on the surface of the sample for the FEM oscillated at around 880 °C, for the laboratory test at 875 °C. On the other hand, in the last case (1150 °C), the maximum temperature on the surface of the sample for the FEM was 950 °C, for the laboratory sample 1025 °C.

After performing laboratory tests and then numerical tests, an analysis of the results obtained (distribution maps of values of principal stresses, minimum stresses, triaxial stresses, mean stresses and reduced strains) was performed.

On the basis of the obtained maps of the distribution of the values of individual parameters, the values for each of the samples were read out at the locations of the 21 measuring sensors along the axis of rotation during forming. In

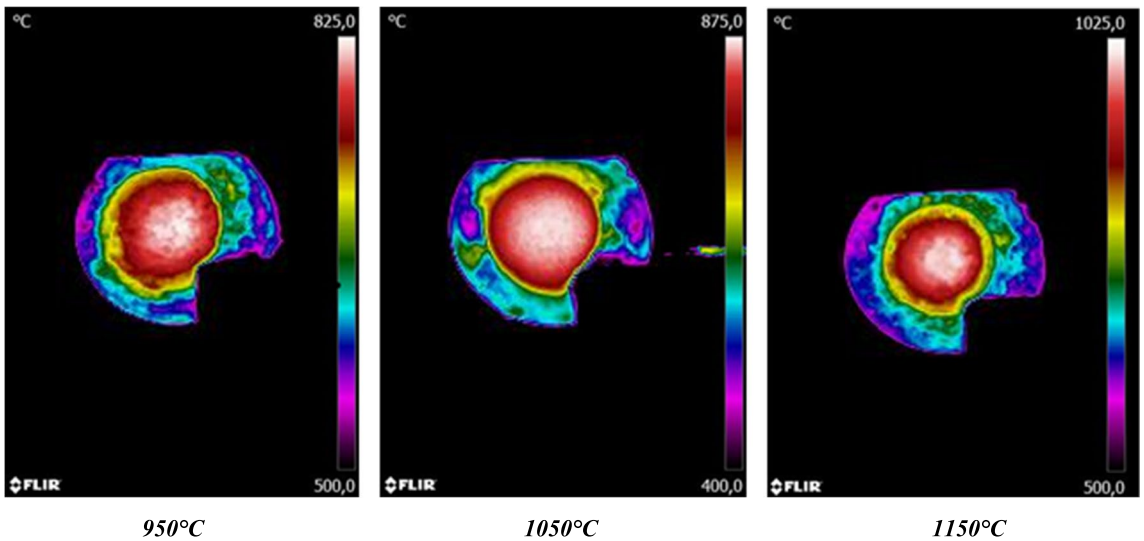

Fig. 9 Map of temperature distribution on the surface of rotary compressed samples

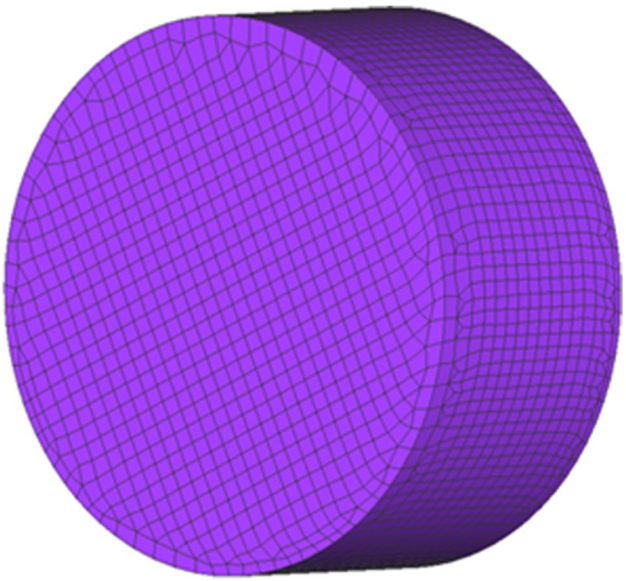

Fig. 10 FEM mesh of the workpiece material

the next step, graphs were produced (Fig. 14) showing the change in the values of the individual parameters along the axis when cracking occurred inside the forming specimen.

In the next stage of the research, on the basis of data obtained from computer simulations, the value of the damage function was calculated according to Pater's hybrid failure criterion [16].

After calculating the value of the hybrid cracking criterion according to Pater along the axis of rotation of the shaped sample, the results are presented in the form of a graph (Fig. 15a), the variation of the criterion value depending on the change in forming temperature at the individual measuring points at the time of cracking.

Once the values of Pater's hybrid cracking criterion had been obtained, a statistical analysis was carried out on the values obtained (Table 3), which were then presented in the graph (Fig. 15b) as a function of the variation of the criterion value as a function of the change in forming temperature of the specimens made from EA1T railway steel.

Statistical analysis of the critical failure value according to Pater's hybrid cracking criterion was carried out using two tests. The first test was the Q-Dixon test. which checks whether a measurement result is very different from the rest of the series. The test counts a Q-factor. which shows how much the suspect value deviates from the rest of the sample. The Q-factor is compared to a critical value. which depends on the number of measurements and the probability of error. If the Q-factor is greater than the critical value. it means that the suspect value is wrong and can be removed. The Q-Dixon test can only be applied to one outlier in a sample.

The second test used is the z-score. which shows whether the score is close to or far from the mean. This test divides the difference between the score and the mean by the standard deviation. The z-score test makes it possible to compare results from different data sets that may differ. The test is also used to check whether averages are equal or different. To calculate the z-score test. we need to know the mean and standard deviation of the dataset to which the score belongs. We use Eq. (4) for the calculation.

$$Z_i = \frac{x_i - \bar{x}}{S} \tag{4}$$

where

xi value to be compared

$\bar{x}$ mean of the population or sample

S standard deviation of the sample or population

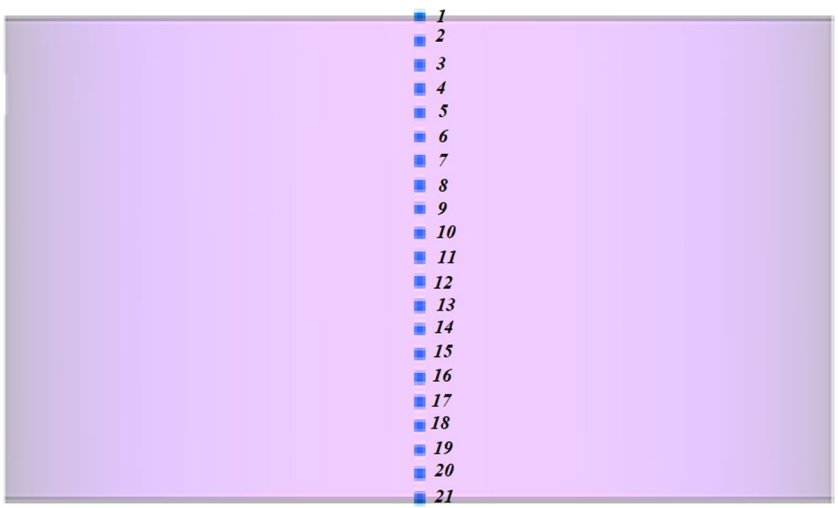

Fig. 11 Measurement points (sensors) marked on the batch axis

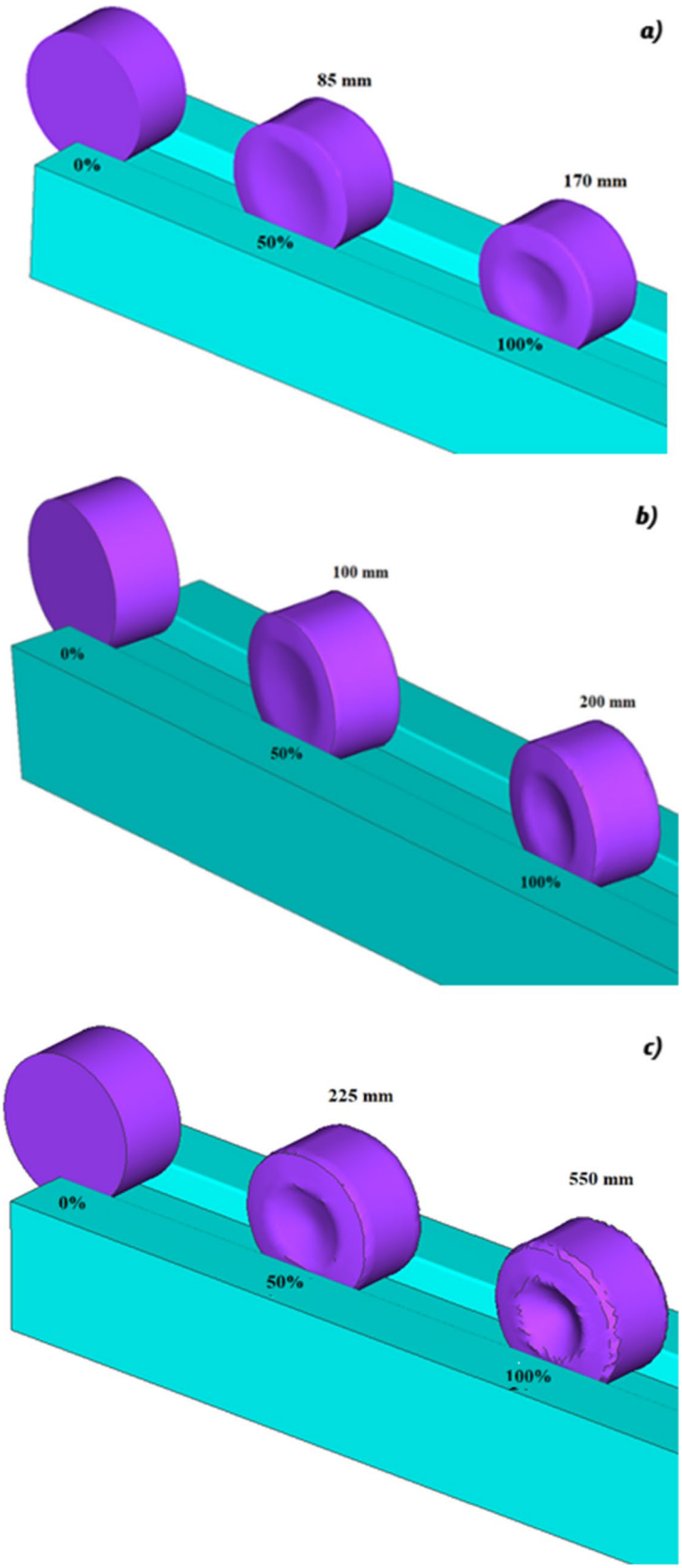

Fig. 12 Shape progression of the sample: **a** 950 °C, **b** 1050 °C, **c** 1150 °C

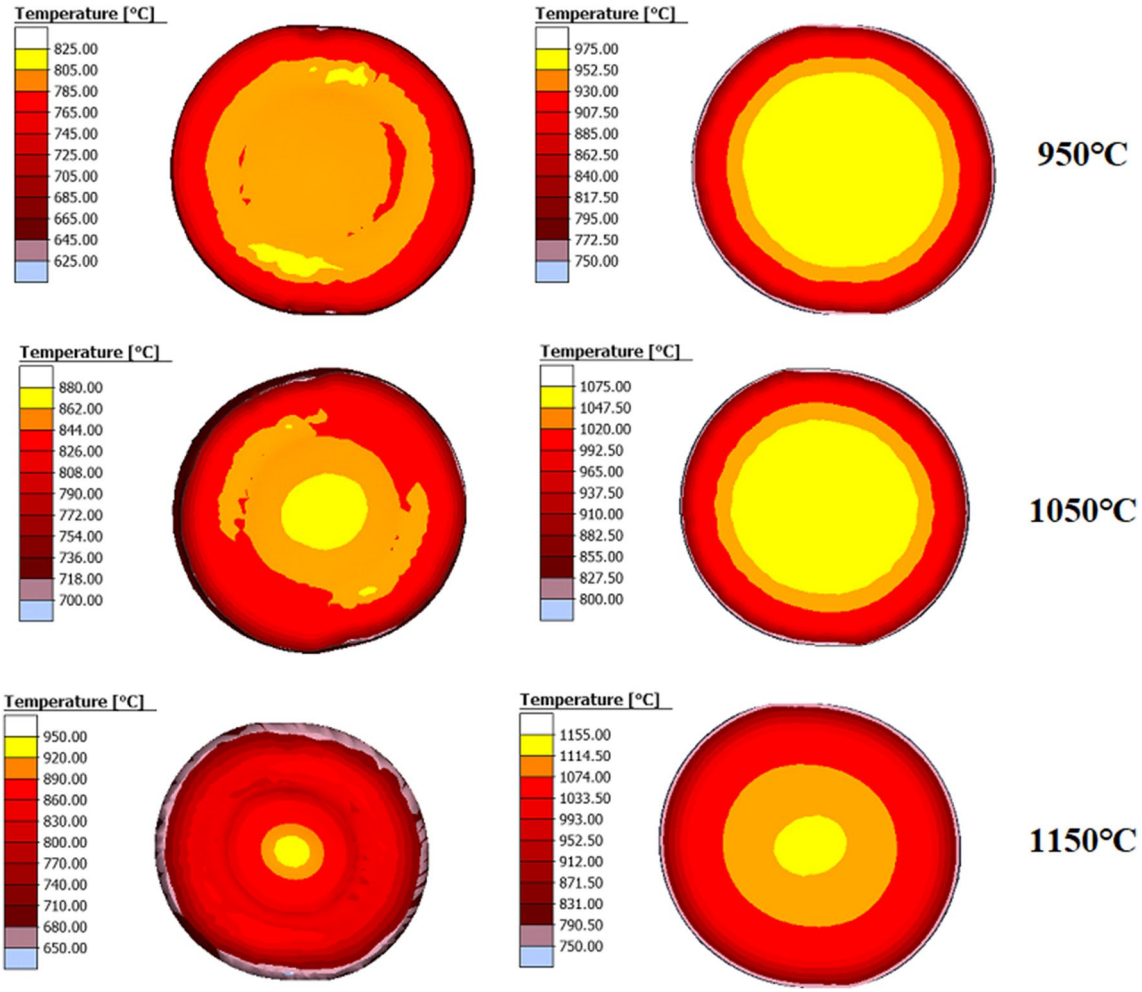

Fig. 13 Temperature distribution at the time of cracking

As a first step in the statistical analysis. it was necessary to determine the mean. minimum. maximum. spread and standard deviation. the values of which are presented in Table 4. The highest standard deviation was observed for the temperature of 950 °C. while the lowest was observed for the highest temperature. In the case of the difference between the maximum and minimum value. the largest was observed at 1150 °C and is greater by about 22.2%. while the smallest difference is at 950 °C and is equal to about 11.2%.

In the case of the Q - Dixon test for temperatures of 950 °C and 1050 °C. the criterion is met by all the values obtained from the 21 measuring sensors. while in the case of shaping samples at 1150 °C. the Q-Dixon test excluded the measurements of sensors 20 and 21.

The Z-score statistical test carried out eliminated the measurements of all forming temperatures in the tests. In the case of tests carried out at 950 °C. the test eliminated the measurement of sensor number 1; in the test of the next case. in which the sample was formed at 1050 °C. the values obtained by sensors numbered 1, 2 and 21 were eliminated; in the case of samples formed at 1150 °C. the z-score test indicated for elimination the values determined by sensors numbered 20 and 21.

For forming specimens at 950 °C. the following critical values of Pater's hybrid cracking criterion were obtained after static analysis: Q-Dixon – 0.7459; Z-Score – 0.7467. For the forming temperature of 1050 °C. the same value was obtained in both tests: 0.8936. On the other hand. forming samples at 1150 °C. the hybrid criterion values were obtained equal to. respectively: : Q-Dixon – 3.1988; Z-Score – 3.1896.

Averaging the results of the two tests. values were obtained: 950 °C – 0.463; 1050 °C – 0.8936; 1150 °C – 3.1942.

Conclusion

The manufacturing technology of wagon axles can significantly influence the safe use of the axles produced. One of the weight-axle manufacturing processes where there is

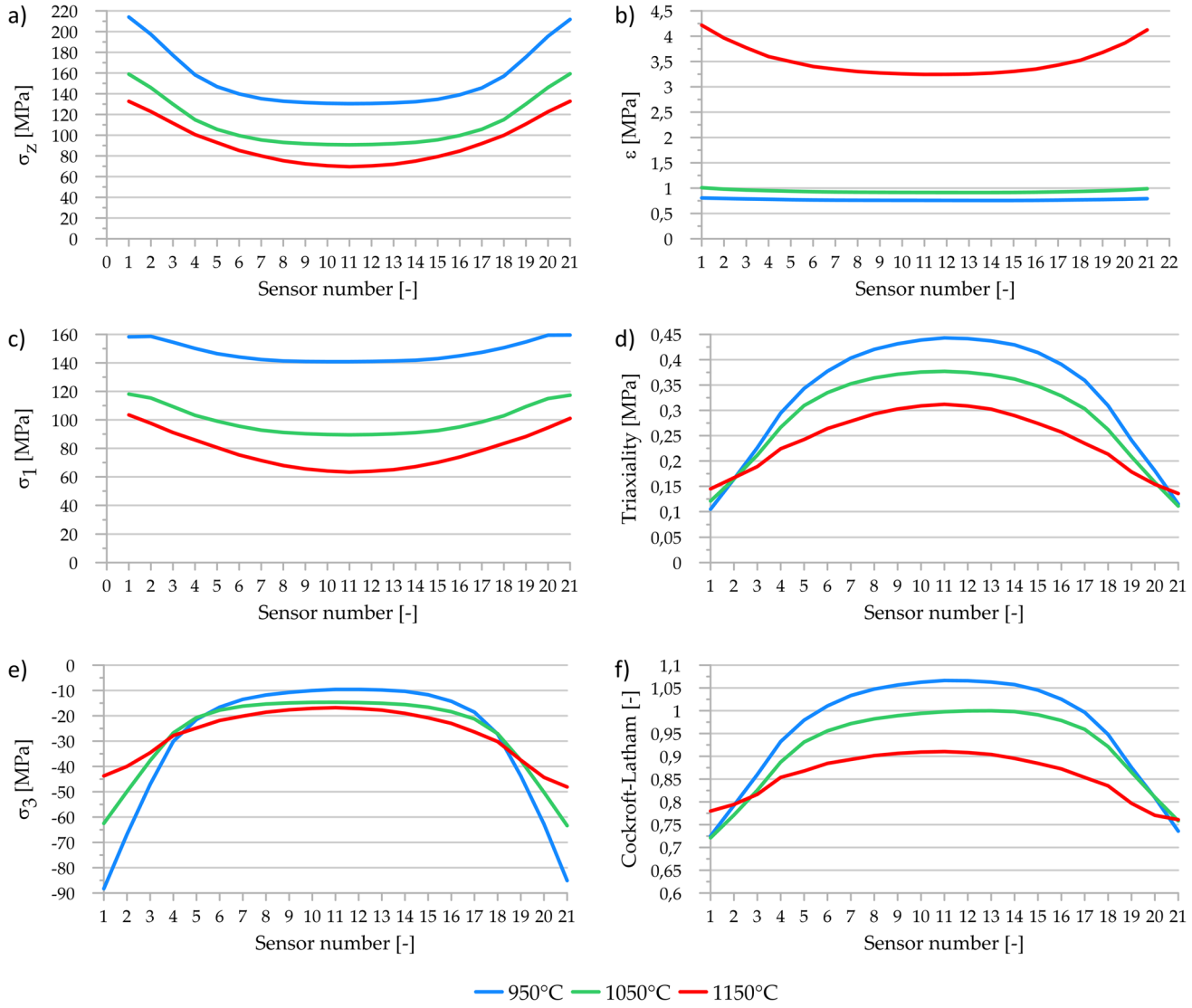

Fig. 14 Graphs of the change in parameter values in the measuring sensors: **a** effective stresses, **b** reduced strains, **c** maximum principal stresses, **d** triaxial stresses, **e** minimum principal stresses, **f** cracking criterion value according to the standardised Cockroft-Latham criterion

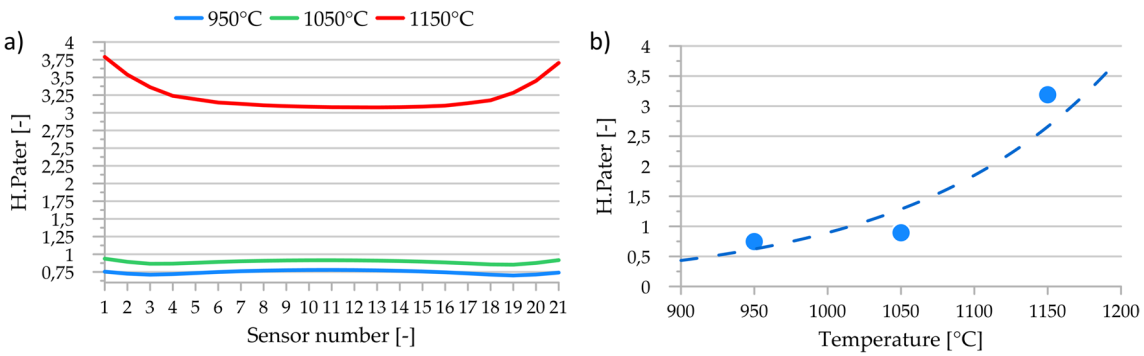

Fig. 15 Values of the hybrid cracking criterion according to Pater for EA1T steel: **a** variation of the criterion value as a function of forming temperature at the measurement points, **b** variation of the Pater cracking criterion value as a function of specimen forming temperature

Table 3 Pater's hybrid cracking criterion values for EA1T steel

Sensor No.	Pater hypothesis		
	950 °C	1050 °C	1150 °C
1	0.7538	0.9376	3.7899
2	0.7254	0.8929	3.5384
3	0.7109	0.8655	3.3619
4	0.7193	0.8671	3.2392
5	0.7342	0.8792	3.1918
6	0.7491	0.8919	3.1450
7	0.7607	0.9012	3.1265
8	0.7686	0.9077	3.1059
9	0.7743	0.9123	3.0941
10	0.7775	0.9149	3.0859
11	0.7786	0.9155	3.0793
12	0.7765	0.9136	3.0777
13	0.7723	0.9099	3.0761
14	0.7658	0.9040	3.0800
15	0.7568	0.8958	3.0879
16	0.7447	0.8846	3.1009
17	0.7291	0.8709	3.1355
18	0.7117	0.8563	3.1765
19	0.7003	0.8528	3.2825
20	0.7131	0.8769	3.4511
21	0.7407	0.9168	3.7053

Table 4 Statistical values of the cracking criterion tests for EA1T steel

	950 °C	1050 °C	1150 °C
Average $\bar{X}$	0.7459	0.8936	3.2348
MIN	0.7000	0.8528	3.0761
MAX	0.7786	0.9376	3.7899
R-distribution	0.0783	0.0848	0.7138
Standard deviation S	0.0248	0.0223	0.2091

one limitation that negatively affects the safety of use is cross-wedge rolling and CNC skew rolling. The limitation is the formation of micro-cracks along the forming axis. which can cause damage or accelerate wear and tear during operation.

The laboratory and numerical tests carried out made it possible to locate the site of cracking and the magnitude of the values according to the hybrid cracking criterion according to Pater using the example of EA1T railway steel.

On the basis of the analysis carried out. it was concluded that:

- The hybrid cracking criterion defines in a good way the locations of post-cracking formation of axisymmetric products. using the example of EA1T railway axle rolling.
- Verification of the numerical studies by carrying out laboratory tests made it possible to determine the correctness of the modified Pater hypothesis.
- Numerical and real tests allowed the determination of cracking criterion values according to the modified patera hypothesis for EA1T steel. obtained from rotary compression tests in the channel. which are respectively for temperatures of 950 °C. 1050 °C and 1150 °C: 950 °C – 0.7463; 1050 °C – 0.8936; 1150 °C – 3.1942.
- The largest increase in the cracking criterion value compared to 950 °C was observed for forming at 1150 °C. which is about 3.3 times higher. while the cracking limit is about 2.5 times higher.
- It was found that the hybrid cracking criterion according to Pater. can be used to predict cracking during the rolling process of wagon axles.

Acknowledgements The research was financed in the framework of the project: Development of new rolling technologies for rail axle forgings, No. LIDER/9/0060/L-12/20/NCBR/2021. Total cost of the Project: 1 466 831.25 PLN. The project is financed by the National Centre for Research and Development under the 12th edition of the LIDER Programme.

Declarations

Conflict of interest The authors declare no conflict of interest.

References

1. Kozevnikova GW, Pipipcuk GP, Rudovic AO, Schukin VJ (2017) Progressive method of production of raw railway axles. Technika Zeleznych Dorog 40:31–37
2. Shu XD, Wei XH, Li CM, Hu ZH (2010) The influence rules of stress about technical parameters on synchronous rolling railway axis with multi-wedge cross-wedge rolling. Appl Mech Mater 37:1482–1488. https://doi.org/10.4028/www.scientific.net/AMM.37-38.1482
3. Romanenko VP, Stepanov PP, Kriskovich SM (2018) Production of hollow railroad axles by screw piercing and radial forging. Metallurgist 61:873–877. https://doi.org/10.1007/s11015-018-0579-0
4. Pater Z (2020) A comparative analysis of forming Railway axles in 3- and 4-Roll Rolling Mills. Materials 13:3084. https://doi.org/10.3390/ma13143084

5. Pater Z (2022) Study of Cross Wedge Rolling Process of BA3002 - Type Railway Axle. Adv Sci Technol Res J 16:225–231. https://doi.org/10.12913/22998624/147310
6. Iwnicki S (2006) Handbook of railway vehicle dynamics (2nd edn). CRC Press
7. Hu B, Shu XD, Yu PH, Peng WF (2014) The strain analysis at the broadening stage of the hollow railway axle by multi-wedge cross wedge rolling. Appl Mech Mater 494:457–460. https://doi.org/10.4028/www.scientific.net/AMM.494-495.457
8. Xu C, Shu XD (2018) Influence of process parameters on the forming mechanics parameters of the three-roll skew rolling forming of the railway hollow shaft with 1: 5. Metalurgija 57(3):153–156
9. Shu X, Ye C, Wang J, Xia Y, Zhang S, Wang Y, Deng Y (2023) Analysis and prospect of precision plastic forming technologies for production of high-speed-train hollow axles. Metals 13(1):145. https://doi.org/10.3390/met13010145
10. Li J (2007) Numerical simulation research on the hollow high-speed railway axle during radical forging (Master's thesis). Taiyuan University of Science and Technology, Taiyuan
11. Huo Y, Huo C, Ren X, He T, Hosseini SRE, Wang B, Cui Y, Jia C, Liu K, Du X (2023) Numerical prediction of microstructure evolution of high-speed railway axle formed using hot cross wedge rolling. Mater Today Commun 35:105985. https://doi.org/10.1016/j.mtcomm.2023.105985
12. Huo Y, Lin J, Bai Q, Wang B, Tang X, Ji H (2017) Prediction of microstructure and ductile damage of a high-speed railway axle steel during cross wedge rolling. J Mater Process Technol 239:359–369. https://doi.org/10.1016/j.jmatprotec.2016.09.001
13. Baiwei C (2006) Radial forging of conical hollow-axis in high speed locomotive. Mech Eng 3:3–5
14. Pater Z (2014) Cross-wedge Rolling. In: Button ST (ed) Comprehensive materials processing. Elsevier Ltd, pp 211–279. https://doi.org/10.3390/ma14216638
15. Pater Z, Tomczak J, Lis K, Bulzak T, Shu X (2020) Forming of rail car axles in a CNC skew rolling mill. Archiv Civ Mech Eng 20:69–82. https://doi.org/10.1007/s43452-020-00075-5
16. Rieger M, Moser C, Brunnhofer P, Simunek D, Weber FJ, Deisl A, Gänser HP, Pippan R, Enzinger N (2020) Crack growth in full-scale railway axles – influence of residual stresses and load sequence effects. Int J Fatig 132:105360. https://doi.org/10.1016/j.ijfatigue.2019.105360
17. Yamamoto M, Makino K, Ishiduka H (2019) Experimental validation of fatigue crack growth of railway axle using operational load. Eng Fract Mech 213:142–152. https://doi.org/10.1016/j.engfracmech.2019.05.011
18. Cervello S (2016) Fatigue properties of railway axles: new results on full-scale specimens from the euraxles project. Int J Fatig 86:2–12. https://doi.org/10.1016/j.ijfatigue.2015.12.003
19. Pater Z, Tomczak J, Bulzak T (2020) Establishment of a new hybrid fracture criterion for cross wedge rolling. Int J Mech Sci 167:105274. https://doi.org/10.1016/j.ijmecsci.2019.105274
20. Jia C, Huo Y, He T, Hosseini SRE, Wu W, Huo C, Wang B (2022) Numerical prediction of ductile damage evolution of 40CrNiMo railway axle steel during hot cross wedge rolling. Mater Today Commun 33:104942. https://doi.org/10.1016/j.mtcomm.2022.104942
21. Anderson TL (2005) Fracture mechanics. Fundamentals and Applications. Taylor & Francis, Boca Raton
22. Lemaitre J, Dasmorat R (2005) Engineering damage mechanics, ductile, creep and brittle failures. Springer, Berlin
23. Hambli R, Reszka M (2002) Fracture criteria identification using an inverse technique method and banking experiment. Int J Mech Sci 44:1349–1361. https://doi.org/10.1016/S0020-7403(02)00049-8
24. Kraišnik M, Vilotič D, Šidanin L, Stefanovič M (2015) Various approaches to defining the criteria of ductile crack in cold bulk forming processes. Int J Eng 13:213–218
25. Fischer FD, Kolednik O, Shan GX, Rammerstorfer FG (1995) A note on calibration of ductile failure damage indicators. Int J Fract 73:345–357
26. Ji H, Liu J, Wang B, Zheng Z, Huang J, Hu Z (2015) Cross-wedge rolling of a 4Cr9Si2 hollow valve: explorative experiment and finite element simulation. Int J Adv Manuf Technol 77:15–26. https://doi.org/10.1007/s00170-014-6363-9
27. Yang C, Ma J, Hu Z (2017) Analysis and design of cross wedge rolling hollow axle sleeve with mandrel. J Mater Process Technol 239:346–358. https://doi.org/10.1016/j.jmatprotec.2016.09.002
28. Jing Z, Xuedao S, Zhenghuan H (2007) Computer aided design for cross wedge rolling tools of automobile semi-axes. J Mater Process Technol 187–188:41–45. https://doi.org/10.1016/j.jmatprotec.2006.11.189
29. Zhou X, Shao Z, Pruncu CI, Hua L, Balint D, Lin J et al (2020) A study on central crack formation in cross wedge rolling. J Mater Process Technol 279:116549. https://doi.org/10.1016/j.jmatprotec.2019.116549
30. Bulzak T, Pater P, Tomczak Z, Wojcik J, Murillo-Marrodán Ł (2022) Internal crack formation in cross wedge rolling: fundamentals and rolling methods. J Mater Process Technol 307:117681. https://doi.org/10.1016/j.jmatprotec.2022.117681
31. Zhou X, Sun C, Wang B, Jiang J (2022) Investigation and prediction of central cracking in cross wedge rolling. Int J Adv Manuf Technol 123:145–159. https://doi.org/10.1007/s00170-022-10126-1